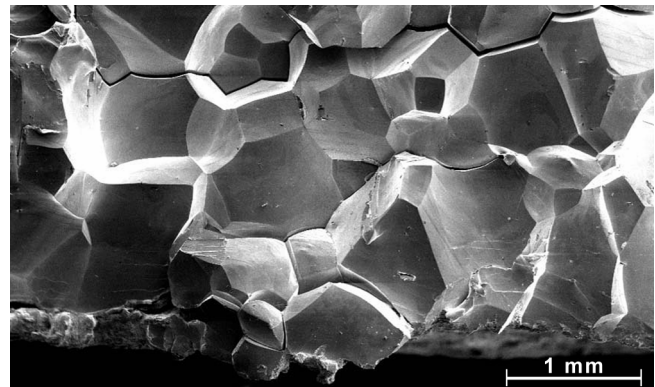




Executive summary

Investigation of a Broken Pile-Shoe from a Roman Bridge



Problem area

A Roman pile-shoe had breaks in three of its four iron bars. One break was recent. The pile-shoe surfaces were also corroded. The breaks were due primarily to brittle intergranular fracture, which is unusual in iron. A collaborative investigation was decided upon.

Description of work

Samples from the pile-shoe were investigated fractographically, metallographically, and by surface and bulk chemical analyses.

Results and conclusions

Samples could be broken into fragments simply by striking with a hammer. This impact brittleness was most probably due to the combination of extremely low carbon and high phosphorus contents. Surface corrosion could have facilitated the brittleness.

Applicability

Similar pile-shoes should be handled with care and should also be protected against further corrosion.

Report no.

NLR-TP-2007-045

Author(s)

R.J.H Wanhill
P.A. Seinen
R.A. Rijkenberg
H.J.M. Meijers

Report classification

Unclassified

Date

January 2007

Knowledge area(s)

Aircraft Material & Damage
Research

Descriptor(s)

pile-shoe
phosphoric iron
brittle fracture
grain boundaries

This report is based on an article to be published in *Historical Metallurgy*, Vol. 41 Part 1, 2007, by the Historical Metallurgy Society.

Investigation of a Broken Pile-Shoe from a Roman Bridge

Nationaal Lucht- en Ruimtevaartlaboratorium, National Aerospace Laboratory NLR

Anthony Fokkerweg 2, 1059 CM Amsterdam,
P.O. Box 90502, 1006 BM Amsterdam, The Netherlands

Telephone +31 20 511 31 13, Fax +31 20 511 32 10, Web site: www.nlr.nl



NLR-TP-2007-045

Investigation of a Broken Pile-Shoe from a Roman Bridge

R.J.H Wanhill, P.A. Seinen¹, R.A. Rijkenberg² and H.J.M. Meijers³

¹ Philips Research Eindhoven: also *Mergor in Mosam*

² Corus RD&T IJmuiden

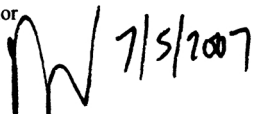
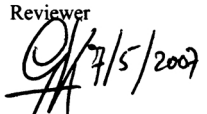
³ Museum Het Valkhof Nijmegen

This report is based on an article to be published in *Historical Metallurgy*, Vol. 41 Part 1, 2007, by the Historical Metallurgy Society.

The contents of this report may be cited on condition that full credit is given to NLR and the author(s).

Customer National Aerospace Laboratory NLR
Contract number
Owner National Aerospace Laboratory NLR
Division Aerospace Vehicles
Distribution Unlimited
Classification of title Unclassified
January 2007

Approved by:

Author  7/5/2007	Reviewer  7/5/2007	Managing department 
---	---	--



Summary

A Roman pile-shoe made from four iron bars had breaks in three bars. One break was a recent impact fracture. A sample containing one of the fracture surfaces was broken into large fragments with a hammer. These were investigated fractographically, metallographically, and by surface and bulk chemical analyses. The fractures were brittle and primarily intergranular. The metal was a coarse-grained phosphoric wrought iron (0.52 wt.% P) with very low silicon, manganese and sulphur contents, and extremely low carbon content (0.0033 wt.% C). The extremely low carbon content and coarse grain size indicate decarburisation during smithing. Furthermore, the combination of extremely low carbon and high phosphorus contents is concluded to be the most probable reason for the impact brittleness. This could have been facilitated by a notch effect due to surface corrosion. The significance of the embrittlement and surface corrosion is considered with respect to conservation of archaeological iron objects, including similar pile-shoes.

Contents

Introduction	4
Experimental scope of the investigation	4
Fractography	5
Metallography	5
Bulk chemical analysis	6
Fracture surface analysis	6
Discussion	7
Carbon content and smithing	8
Carbon content and segregation-induced brittleness	8
Phosphorus and manganese contents and smithing	9
Cause of embrittlement	10
Conservation of other pile-shoes	10
Conclusions	11
Acknowledgements	11
References	11

2 Tables
13 Figures

Introduction

Obstacles in the Maas riverbed, near the town of Cuijk in the Netherlands, were recognised in the early 1990s to be the remains of a Roman bridge. An archaeological recovery programme was set up (Goudswaard 1996; Goudswaard *et al.* 2000), with the primary assistance of divers from the amateur archaeological organisation *Mergor in Mosam* (MiM). The recovery programme resulted in finding many stone blocks and more than 100 oak piles. The remains of the piles were 2–3m long, 30–40cm square above the pointed lower ends, and some were still covered at these ends by iron pile-shoes, see figure 1. The piles (and hence the pile-shoes) have been dated to the 4th century AD. Dendrochronological investigations of the wooden piles showed that the bridge was built in three stages between 340AD and 400AD (Haalebos *et al.* 2002). Figure 2 illustrates the bridge construction: the bridge was supported by stone columns built on top of the wooden piles, which had been driven into the riverbed.

Each pile-shoe was made from four iron bars, joined by heating and hammer-welding to form a point. The bars had approximate dimensions of 13×40×500 mm. One pile-shoe was observed to have three broken bars, and at least one break was recent. This was an impact fracture owing to the pile-shoe falling onto the floor of a storage area. MiM sent the pile-shoe to the museum “Het Valkhof” for initial examination. Figure 3 shows the breaks and a sawn-off slice containing the upper fracture surface of the recent break. Figure 4 shows the lower fracture surface. Over the centuries in the riverbed the bar had corroded to varying depths, up to about 0.5mm; the largely internal fracture had shiny facets, some of which were up to 3mm in size. This unusual and obviously brittle fracture prompted a detailed investigation.

Experimental scope of the investigation

The sawn-off slice shown in figure 3 was struck on a side surface by a hammer, resulting in brittle fracture into large fragments. These fragments were then used for the investigation summarised in table 1. This “sampling”, though highly unorthodox, was effective and confirmed the ambient temperature impact brittleness of the bar.

As the results accumulated, it became clear that *fresh* fracture surfaces should be examined, if possible, for evidence of elemental (phosphorus) segregation to grain boundaries. Unfortunately, specimens could not be made for *in vacuo* fracture and examination by Auger Electron Spectroscopy (AES). The alternative was to break a sample in a nominally inert atmosphere and investigate the fracture surface by XPS.

Fractography

Figure 4 shows the macrofractographic appearance of the recent break, already discussed in the introduction. Figures 5 and 6 are FEG-SEM fractographs of a sample obtained from the sawn-off slice. These show brittle intergranular and cleavage fracture. Intergranular fracture predominated at, and near, the outside surfaces. The grain size varied from about 0.25mm to more than 2mm, which is very coarse.

Metallography

Metallography was done on two samples. The first sample was used to examine the microstructure, iron and inclusion compositions and hardness. Figure 7 and table 2 summarise the results for the iron matrix. The microstructure after polishing and etching with Nital showed large undeformed ferrite grains, with an unusual etching effect in Zones 2 and 3. This etching effect is due to phosphorus segregation and typically occurs in ancient phosphoric iron (Stewart *et al.* 2000b; Godfrey *et al.* 2003; Godfrey 2005). Other images consistently showed the same three zones, which are undoubtedly the result of hot-welding three strips of iron together to form the bar.

The EPMA+WDX measurements in table 2 show that the metal was a phosphoric iron with very low manganese and sulphur contents. These results are consistent with an ancient origin, i.e. they are what would be expected from smelting a phosphorus-containing iron ore in a furnace fuelled by charcoal rather than cokes. The hardness values are typical for annealed phosphoric irons (Tylecote 1986, p.145): note that the fracture location was not involved in the final making of the pile-shoe, since it was about 10cm from the weld area, see figure 3.

Figure 7 also shows deformation twins and a few elongated or ovoid inclusions in Zones 1 and 3. Figure 8 is another image of Zones 2 and 3, showing twins and inclusions in Zone 3 and the unusual etching effect in more detail. The twins, which are the sharp lines confined to the near-surface regions, are the result of the hammer blow to obtain the sample. Some of the inclusions were analysed and found to contain iron, phosphorus and oxygen.

Another area of this first sample had much larger elongated inclusions in Zone 1. These contained predominantly iron, oxygen and silicon, and also aluminium, calcium, magnesium, phosphorus, potassium and sodium. They were probably the remains of smelting slag that had not been fully removed during smithing the iron bloom and subsequent smithing of the wrought

iron stock. Similar slag inclusions were reported for a pile-shoe from the Roman bridge at Minturnae (Campbell and Fahy 1984).

The second sample was used for three EPMA line scans of phosphorus and oxygen contents across grain boundaries, as indicated in figure 9 and illustrated in figure 10. There were no indications of pronounced segregation of either phosphorus or oxygen at the grain boundaries. In total, the line scans showed phosphorus contents varying between 0.2 wt.% and 0.44 wt.%, which agrees well with the data in table 2. The oxygen contents varied between 0.17 wt.% and 0.44 wt.%.

Bulk chemical analysis

The XRF and Combustion + IR bulk analyses on another sample gave the following results: 0.06 wt.% Si ; 0.52 wt.% P ; 0.01 wt.% Mn ; 0.004 wt.% S ; 0.0033 wt.% C ; with the balance nominally being 99.4 wt.% Fe (oxygen content was not determined). The analyses are consistent with the EPMA+WDX results, table 2. The extremely low carbon content is important, as will become clear in the discussion section.

An XRD bulk analysis was also done for the corroded surface of a sample and a clean fracture surface. The corrosion layer closest to the metal surface was identified as akaganeite, while the fracture surface was virtually pure ferritic iron. The identification of akaganeite is important. It forms after excavation, when oxygen gets unhindered access to the wet corrosion layer (Selwyn 2004), which must contain chloride ions (Balasubramaniam *et al.* 2003; Neff *et al.* 2005). Since iron chloride is hygroscopic, the corrosion on the pile shoe will probably continue unless preventative measures are taken.

Fracture surface analysis

XPS was used to look for evidence of elemental (phosphorus or oxygen) segregation on grain boundary fracture facets. A saw-notched new sample was inserted into a glove box in an atmosphere of nitrogen containing 0.1ppm H₂O and 0.3ppm O₂. The sample was then broken and one fracture surface transferred directly to the vacuum chamber of the XPS equipment.

Figure 11 shows a Secondary X-ray Image (SXI) of the measurement positions on the fracture surface, whereby it was intended to analyse grain boundary facets only (however, post-analysis SEM fractography showed that the fracture surface consisted mainly of cleavage facets). Depth

profiles of elemental concentrations were obtained from measurements using monochromatic Al K α radiation, spot size 100 μ m, alternating with argon sputtering. Figure 12 gives a representative result. Only iron and oxygen were detected, with a very high oxygen concentration on the initial fracture surface and persistent oxygen concentrations \approx 12 at.% (3.5 wt.%) after sputtering times of 2–15 minutes. This result must have been due to contamination of the fracture surface by adsorbed oxygen, since otherwise it would signify large amounts of FeO in the bulk metal, and this is inconsistent with the metallography and EPMA+WDX line scan analyses.

Discussion

The metallography and chemical analyses show that the recently broken bar is a phosphoric iron with very low silicon, manganese and sulphur contents; and extremely low carbon content *at the fracture location*. For comparison, analysis of the weld area of a pile-shoe from the Roman bridge at Trier gave the following results: 0.03–0.06 wt.% Si ; 0.21–0.22 wt.% P ; 0.01 wt.% Mn ; 0.008–0.009 wt.% S ; 0.07–0.11 wt.% C (Cüppers 1969, p. 211).

The caveat about the carbon content at the fracture location is because metallographically examined pile-shoes have shown a range of iron microstructures, ranging from ferrite to predominantly pearlite (Cüppers 1969, p. 210; Campbell and Fahy 1984), i.e. varying widely in carbon content.

In contrast, both pile-shoes had very low manganese and sulphur contents despite the very different analysis locations. These results indicate iron ore smelting with charcoal, rather than post-18th century smelting with cokes, i.e. the iron is not of modern origin. Of course, it was already mentioned that the Cuijk piles and pile-shoes date from the 4th century AD. The Trier piles and pile-shoes date from the 2nd century AD.

The iron ore would most probably have been local and locally smelted. Phosphorus-containing bog iron ores were widely available and used for making bloomery iron in the region now known as the Netherlands (Joosten 2004; Godfrey and van Nie 2004). The likelihood of local iron production would not have depended on the different smelting techniques employed within the Roman Empire and by contemporary Germanic people, since the main differences were in the method of slag separation from the iron bloom. The latter aspect is discussed by Godfrey and van Nie (2004).



The carbon content (0.0033 wt.%) of the recently broken bar is important with respect to the smithing of the iron and its present impact brittleness, discussed in the following subsections.

Carbon content and smithing

Together with the large ferrite grain sizes, up to 2–3 mm, the extremely low carbon content of the recently broken bar suggests that decarburising conditions pertained during smithing (Dinnetz 2003), specifically at the fracture location and during heating in a forge in order to hammer-weld the four bars to form the pile-shoe point. Actually, there would have been several smithing steps, starting with the cut-up iron bloom and continuing with forging the iron into bars and strips, welding strips into bars, and welding four bars together to make the pile-shoe. Any or all of these steps could have contributed to reducing the carbon content.

The alternative is that the original iron bloom was extremely low in carbon. There is a strong tendency for high-phosphorus ancient iron to be low in carbon, with carbon contents in the range 0.01–0.1 wt.% (Tylecote 1986, pp. 145,149,151,169). This range in carbon content is significantly above the 0.0033 wt.% of the recently broken bar, suggesting that it is more likely that smithing resulted in the extremely low carbon content.

Be that as it may, the fact that the bar, and presumably others like it, was used for making a pile-shoe shows that the strength was adequate despite the extremely low carbon content. As Tylecote states, there is no reason why a smith working a high-phosphorus iron should be dissatisfied with the strength of the product, since phosphorus will harden iron almost as much as carbon. Smiths would have known that this kind of iron was readily hot-worked and did not require special forging skills. They would also know that it was difficult to cold-work, which is why, in general, there seems to have been a move away from high phosphorus iron ores during the Roman period (Tylecote 1986, p.169). However, they might not have recognised any tendency for the cold iron outside the weld area to be very brittle under impact loading. This is further discussed in the subsection on the cause of embrittlement.

Carbon content and segregation-induced brittleness

Modern metallurgy has shown that the effects of carbon and phosphorus on the mechanical properties of iron alloys are linked (Hopkins and Tipler 1958; Erhardt and Grabke 1981). If phosphorus is present in unalloyed iron it will tend to segregate to the ferrite grain boundaries, resulting in brittle fracture, particularly under impact loading (Inman and Tipler 1958; Hopkins and Tipler 1958; Ramasubramanian and Stein 1973; Erhardt and Grabke 1981). However, carbon can displace phosphorus from the grain boundaries, even if the bulk concentration of phosphorus is relatively high (Hopkins and Tipler 1958; Erhardt and Grabke 1981). This is called the *site-competition effect*, and explains why modern unalloyed carbon steels, which

generally contain no more than 0.15 wt.% phosphorus, are not embrittled. Only if the carbon content is unusually low can phosphorus embrittle the grain boundaries (Erhardt and Grabke 1981).

Besides phosphorus, oxygen can cause intergranular brittle fracture in irons having carbon contents less than 0.005 wt.% (Rees and Hopkins 1952; Kumar and Raman 1981), and has also been shown to segregate to grain boundaries (Kumar and Raman 1981). As in the case of phosphorus, the site-competition effect between carbon and oxygen should play an important role (Krasko 1997).

Very low carbon contents are thus required for segregation-induced embrittlement by phosphorus or oxygen. Since fracture surface analysis by AES was not possible, and the XPS results are inconclusive, the question remains whether to attribute brittle intergranular fracture of the pile-shoe bar to grain boundary segregation of phosphorus or oxygen.

The many tensile and impact test results in the literature are complicated by different heat treatments, testing temperatures, notch effects and qualitative assessments of the fracture characteristics. On the whole, it appears that phosphorus is a more potent embrittler of iron than oxygen, though this does not necessarily mean that fracture is intergranular, since cleavage and partial ductile fracture can also occur.

However, there is one observation that favours phosphorus-induced embrittlement of the pile-shoe bar, namely that oxygen-induced intergranular fracture requires the iron to have a high yield strength (Kumar and Raman 1981). As stated earlier, the hardness values in table 2 are typical for annealed phosphoric irons. These hardnesses suggest low yield strengths in the range 250–350 MPa, see Gale and Totemeier (2004) and Stewart *et al.* (2000a).

Phosphorus and manganese contents and smithing

As mentioned earlier, figure 7 shows that the unusual etching effect was confined to zones 2 and 3. Table 2 shows that these zones had lower phosphorus and higher manganese contents than zone 1. Since phosphorus stabilizes the α -iron phase and manganese stabilizes the γ -iron phase, these metallographic and compositional correlations might reflect the extent to which the three zones were heated into the $(\alpha + \gamma)$ or γ phase fields during the final smithing process.

As a first approximation, the bar material illustrated in figure 7 can be considered as a binary alloy of iron and phosphorus. From figure 13 (Okamoto 1993) we may infer that in order to transgress the $\alpha/(\alpha + \gamma)$ phase boundary this bar material would have had to reach temperatures above 935°C and probably above 1000°C: the position of the $\alpha/(\alpha + \gamma)$ phase boundary is

uncertain. The higher the temperature, the more likely that the material would have a large final (ferrite) grain size, as observed, and already mentioned with respect to carbon content and smithing.

Cause of embrittlement

The results of modern metallurgical research and the present investigation lead us to conclude that the most probable reason for brittleness of the recently broken bar of the pile-shoe is the local combination of extremely low carbon content and high phosphorus content. Obviously, the brittleness did not manifest itself when the pile-shoe was made and subsequently attached to an oak pile. Two possible reasons can be given. Firstly, there would have been no reason to apply impact forces directly to the bar during its attachment, which was done using a nail driven through a hole in the bar, see the lower R.H. corner of figure 3. Secondly, the surface of the bar would have been smooth, which is no longer the case, owing to surface corrosion. Over the intervening centuries the corrosion penetrated up to about 0.5 mm into the bar, and figure 4 shows that the depth of corrosion was not uniform. There could thus have been a notch effect added to the impact force caused by the pile-shoe falling to the floor during storage, and this combination could have facilitated the brittle fracture.

Once intergranular cracking began, the cracks would be subject to dynamic effects, i.e. the crack velocity would contribute to the brittleness. This is possibly why there was a transition to a mixture of intergranular and cleavage fracture in the interior of the bar.

Conservation of other pile-shoes

There are two aspects to conserving other pile-shoes. Firstly, the presence of akaganeite closest to the metal surface suggests that corrosion will continue unless prevented by drying out the corrosion layer and storing the pile-shoes in a low-humidity environment (Selwyn 2004) or applying a protective (organic) coating.

Secondly, the pile-shoe's brittleness needs to be considered in the context of conservation of archaeological iron objects. As mentioned above, ancient phosphoric irons have carbon contents typically in the range 0.01–0.1 wt.% (Tylecote 1986). These amounts of carbon should prevent the type of impact embrittlement shown by the pile-shoe, as may be concluded from impact tests on phosphoric iron and steel containing 0.01–0.015 wt.% carbon (Josefsson 1954; Suzuki *et al.* 1985)¹. Even so, some or many of the other pile-shoes stored in Cuijk could have extremely low carbon contents at similar locations outside the weld area. If any are to be

¹ Carbon-containing phosphoric irons can be embrittled (Rellick and McMahon 1974; Stewart *et al.* 2000a), but this requires specific heat-treatments unlikely to have been employed in antiquity for “everyday” iron objects. See also Gouthama and Balasubramaniam (2003).

removed from storage, they should be handled and transported with care to avoid breakage, despite their fairly robust appearance.

Be that as it may, it would be most interesting to take samples from some of the pile shoes, and from different locations, for chemical analysis, controlled impact testing, fractography and metallography. Further insights into the techniques for manufacturing what is essentially a low-quality, mass-produced artefact would surely be obtained.

Conclusions

Impact brittleness of the pile-shoe bar was most probably caused by the combination of extremely low carbon and high phosphorus contents. Surface corrosion could have facilitated the brittleness by providing a notch effect during impact. The extremely low carbon content and the coarse grain size are most probably due to decarburisation during smithing, though a high heating temperature could also favour coarse grains. Similar pile-shoes should be handled and transported with care, and also protected against further corrosion.

Acknowledgements

We thank *Mergor in Mosam* for supplying the pile-shoe for investigation; A. Hendriks, C. van der Marel, H.J. Wondergem (PR-MA), N. Steenstra, F. Twisk (CORUS), and M. Hogendorn (NLR) for technical assistance; and E.G. Godfrey (University of Mary Washington) for particularly helpful discussions.

References

Balasubramaniam R, Ramesh Kumar A V and Dillmann P 2003, 'Characterization of rust on ancient Indian iron', *Current Science* 85, 1546-1555.

Campbell J and Fahy F 1984, 'A metallurgical study of iron pile shoes from the Roman bridge at Minturnae', *Historical Metallurgy* 18, 21-30.

Cüppers H 1969, *Die Trierer Römerbrücken*, Band V (Mainz am Rhein).

Dinnetz M K 2003, 'Technical and archaeological investigation of an early iron sword from Sweden', in L N Nørbach (ed), *Prehistoric and Medieval Direct Iron Smelting in Scandinavia and Europe, Aspects of Technology and Society* (Aarhus), 101-109.

Erhardt H and Grabke H J 1981, 'Equilibrium segregation of phosphorus at grain boundaries of Fe-P, Fe-C-P, Fe-Cr-P, and Fe-Cr-C-P alloys', *Metal Science* 15, 401-408.

Gale W F and Totemeier T C (eds) 2004, *Smithells Metals Reference Book* (Oxford), 21-4, 22-99-102.

Godfrey E G 2005, *Personal Communication*, Department of Archaeological Sciences, University of Bradford.

Godfrey E G and Van Nie M 2004, 'A Germanic ultrahigh carbon steel punch of the Late Roman-Iron Age', *Journal of Archaeological Science* 31, 1117-1125.

Godfrey E G, Vizcaino A and McDonnell J G 2003, 'The role of phosphorus in early ironworking', in L N Nørbach (ed), *Prehistoric and Medieval Direct Iron Smelting in Scandinavia and Europe, Aspects of Technology and Society* (Aarhus), 191-193.

Goudswaard B 1996, 'Brug te water, Romeinse resten bij Cuijk', *Natuur & Techniek* 64(1), 30-41.

Goudswaard B, Kroes R A C and Van der Beek H S M 2000, 'The Late Roman bridge at Cuijk', *Proceedings of the National Service for Archaeological Heritage in the Netherlands* 44, 440-560.

Gouthama and Balasubramaniam R 2003, 'Alloy design of ductile phosphoric iron: Ideas from archaeometallurgy', *Bulletin of Materials Science* 26, 483-491.

Haalebos J K, Goudswaard B, Kroes R A C and Van der Beek H 2002, 'De laat Romeinse tijd', in H Enkevort and J Thijssen (eds), *Cuijk, een Regionaal Centrum in de Romeinse Tijd* (Utrecht), 80-95.

Hopkins B E and Tipler H R 1958, 'The effect of phosphorus on the tensile and notch-impact properties of high-purity iron and iron-carbon alloys', *Journal of the Iron and Steel Institute* 188, 218-237.

Inman M C and Tipler H R 1958, 'Grain-boundary segregation of phosphorus in an iron-phosphorus alloy and the effect upon mechanical properties', *Acta Metallurgica* 6, 73-84.

Josefsson A 1954, 'Pearlite-free Bessemer steel: its fabrication and properties', *Journal of the Iron and Steel Institute* 177, 118-128.

Joosten I 2004, *Technology of Early Historical Iron Production in the Netherlands* (Amsterdam).

Krasko G L 1997, 'Effect of impurities on the electronic structure of grain boundaries and intergranular cohesion in iron and tungsten', *Materials Science and Engineering A234-236*, 1071-1074.

Kumar A and Raman V 1981, 'Low temperature intergranular brittleness of iron', *Acta Metallurgica* 29, 1131-1139.

Neff D, Dillmann P, Bellot-Gurlet L and Beranger G 2005, 'Corrosion of iron archaeological artefacts in soil: characterisation of the corrosion system', *Corrosion Science* 47, 515-535.

Okamoto, H (ed) 1993, *Phase Diagrams of Binary Iron Alloys* (Materials Park), 311.

Ramasubramanian P V and Stein D F 1973, 'An investigation of grain-boundary embrittlement in Fe-P, Fe-P-S, and Fe-Sb-S alloys', *Metallurgical Transactions* 4, 1735-1742.

Rees W P and Hopkins B E 1952, 'Intergranular brittleness in iron-oxygen alloys', *Journal of the Iron and Steel Institute* 172, 403-409.

Rellick J R and McMahon Jr C J 1974, 'Intergranular embrittlement of iron-carbon alloys by impurities', *Metallurgical Transactions* 5, 2439-2450.

Selwyn L 2004, *Metals and Corrosion: A Handbook for the Conservation Professional* (Ottawa).

Stewart J W, Charles J A and Wallach E R 2000a, 'Iron-phosphorus-carbon system Part 1 – Mechanical properties of low carbon iron-phosphorus alloys', *Materials Science and Technology* 16, 275-282.

Stewart J W, Charles J A and Wallach E R 2000b, 'Iron-phosphorus-carbon system Part 3 – Metallography of low carbon iron-phosphorus alloys', *Materials Science and Technology* 16, 291-303.

Suzuki S, Obata M, Abiko K and Kimura H 1985, 'Role of carbon in preventing the intergranular fracture in iron-phosphorus alloys', *Transactions of the Iron and Steel Institute of Japan* 25, 62-68.

Tylecote R F 1986, *The Prehistory of Metallurgy in the British Isles* (London).

Table 1 Scope of the investigation

Topic	Institute/Organisation	Specific Aspects
Fractography <ul style="list-style-type: none"> Macrofractography SEM / FEG-SEM 	"Het Valkhof" PR-MA / NLR	brittle fracture, corrosion intergranular + cleavage fracture
Optical metallography	CORUS, NLR	microstructure, hardness
Chemical analysis <i>Bulk</i> <ul style="list-style-type: none"> XRD XRF Combustion + IR <i>Metallographic surfaces</i> <ul style="list-style-type: none"> SEM+EDX, EPMA+WDX <i>Fracture surfaces</i> <ul style="list-style-type: none"> XPS 	PR-MA CORUS CORUS CORUS / PR-MA PR-MA	iron and corrosion product iron composition carbon and sulphur content of iron iron and inclusion compositions, phosphorus and oxygen line scans grain boundary segregation

SEM: Scanning Electron Microscope; FEG-SEM: Field Emission Gun SEM; XRD: X-Ray Diffraction; XRF: X-Ray Fluorescence spectroscopy; IR: InfraRed detection; EDX: Energy Dispersive analysis of X-rays; EPMA: Electron Probe MicroAnalysis; WDX: Wavelength Dispersive analysis of X-rays; XPS: X-ray Photoelectron Spectroscopy

Table 2 Iron composition and Vickers microhardness, H_V , for the zones in figure 7

Zone	EPMA+WDX weight % (5 measurements per zone)	H_V (1 kg load)
1	Fe 98.75-99.68; P 0.45-0.52; Si 0.06-0.07; Mn 0.002max; S 0.010max	169, 171, 194
2	Fe 98.92-99.44; P 0.25-0.40; Si 0.05-0.07; Mn 0.013max; S 0.012max	141, 143, 150
3	Fe 98.55-99.07; P 0.28-0.40; Si 0.06-0.07; Mn 0.014max; S 0.009max	144, 155, 159



Figure 1 Some of the piles, pile-shoes and stone blocks recovered from the Maas riverbed: photograph courtesy of R. Kroes

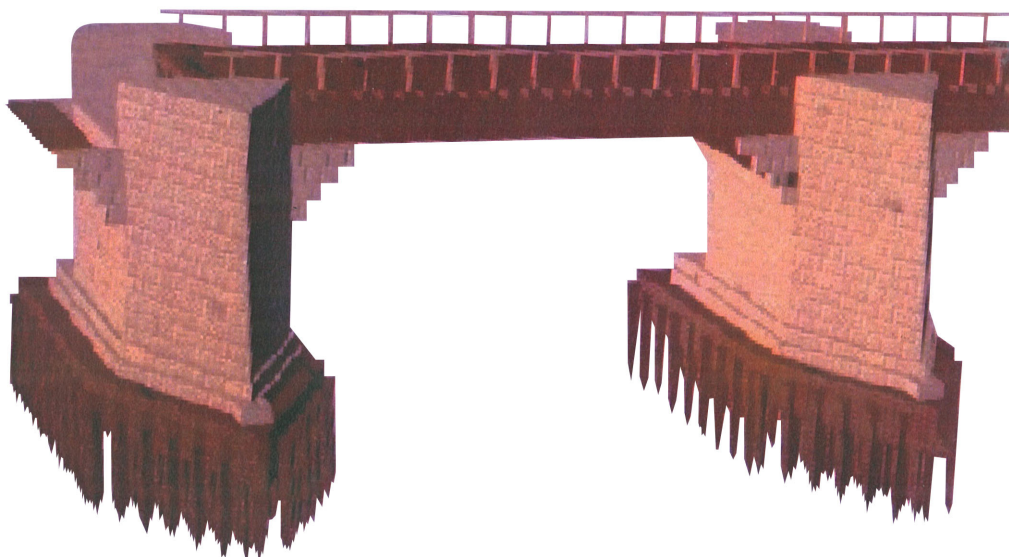


Figure 2 Illustration of the bridge construction



Figure 3 The broken pile-shoe with a sawn-off slice containing the upper fracture surface of the recent break. "N" indicates the head of a nail driven through a hole in the bar in order to attach it to the wooden pile

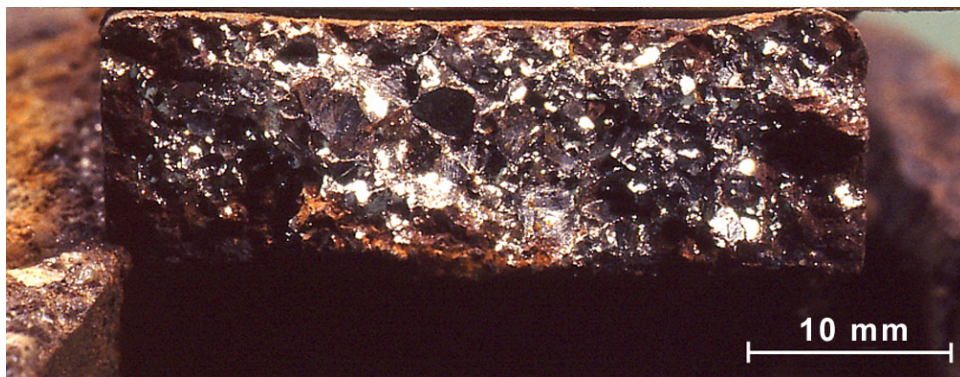


Figure 4 The lower fracture surface of the recent break



Figure 5 FEG-SEM fractograph at, and near, the external surface of a sample from the sawn-off slice. The fracture is almost entirely intergranular

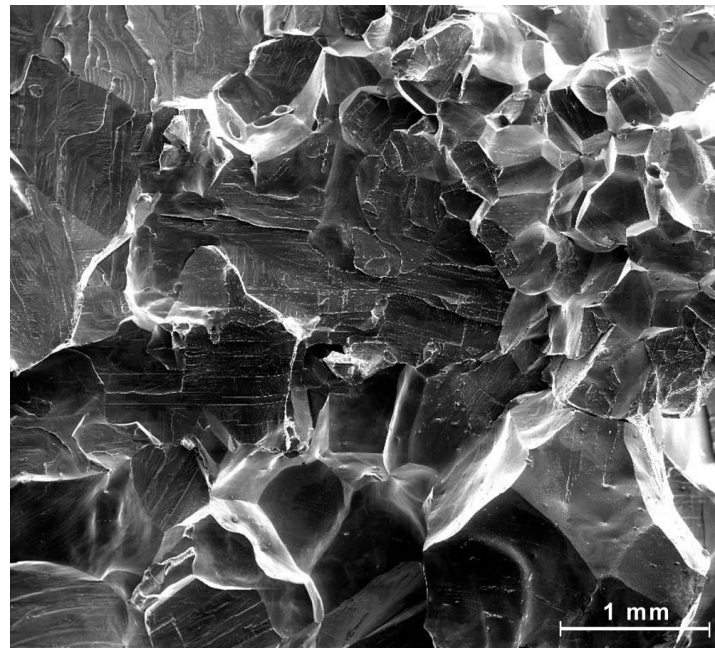


Figure 6 FEG-SEM fractograph nearer the centre of a sample from the sawn-off slice. The fracture is mixed intergranular and cleavage

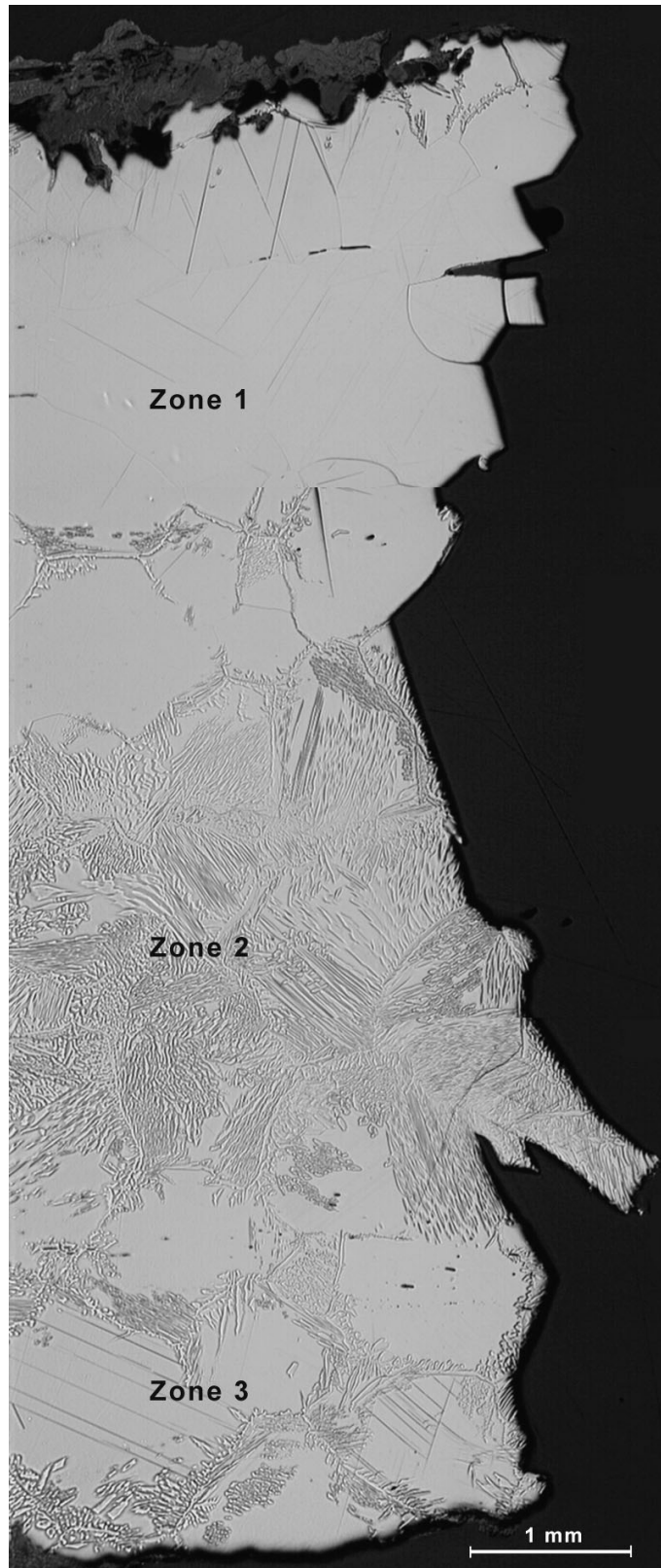


Figure 7 Through-thickness microstructure of a broken sample: the top and bottom edges are the original surfaces. Iron composition and hardness are given in table 2

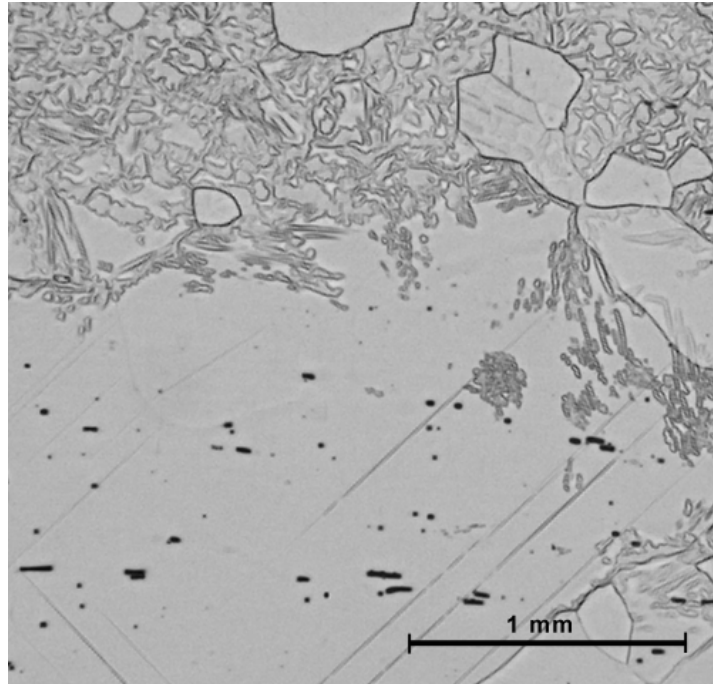


Figure 8 Detail of the microstructure in Zones 2 and 3, showing deformation twins and elongated inclusions in Zone 3 and the unusual etching effect

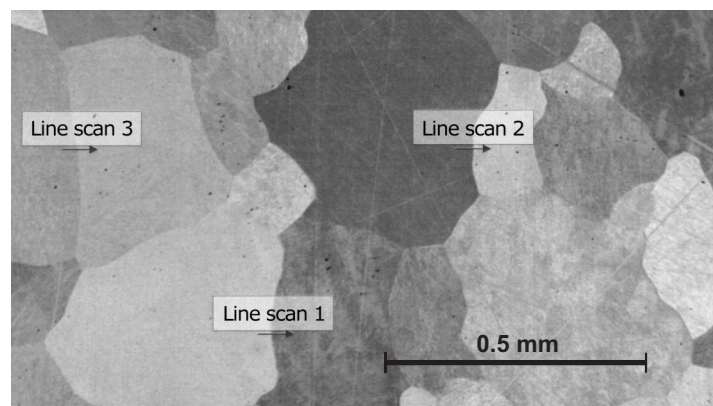


Figure 9 Positions of three EPMA + WDX line scans for phosphorus and oxygen contents

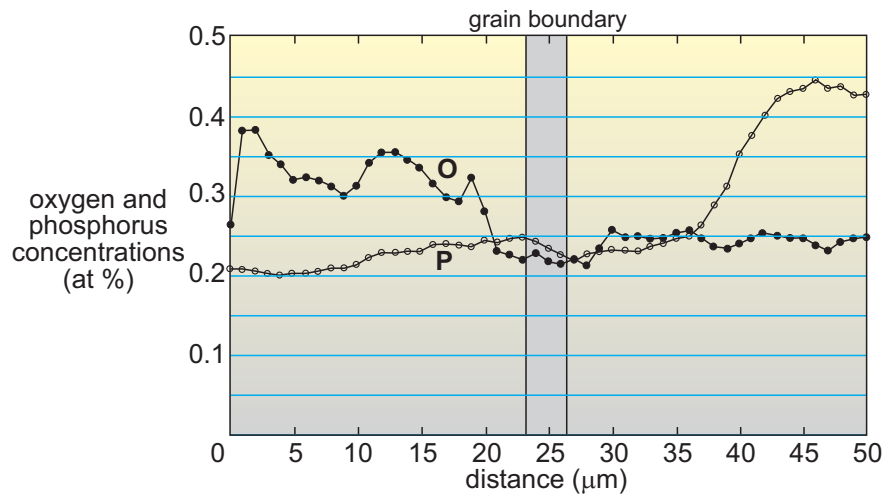


Figure 10 Example EPMA + WDX linescan (position 2 in figure 9)

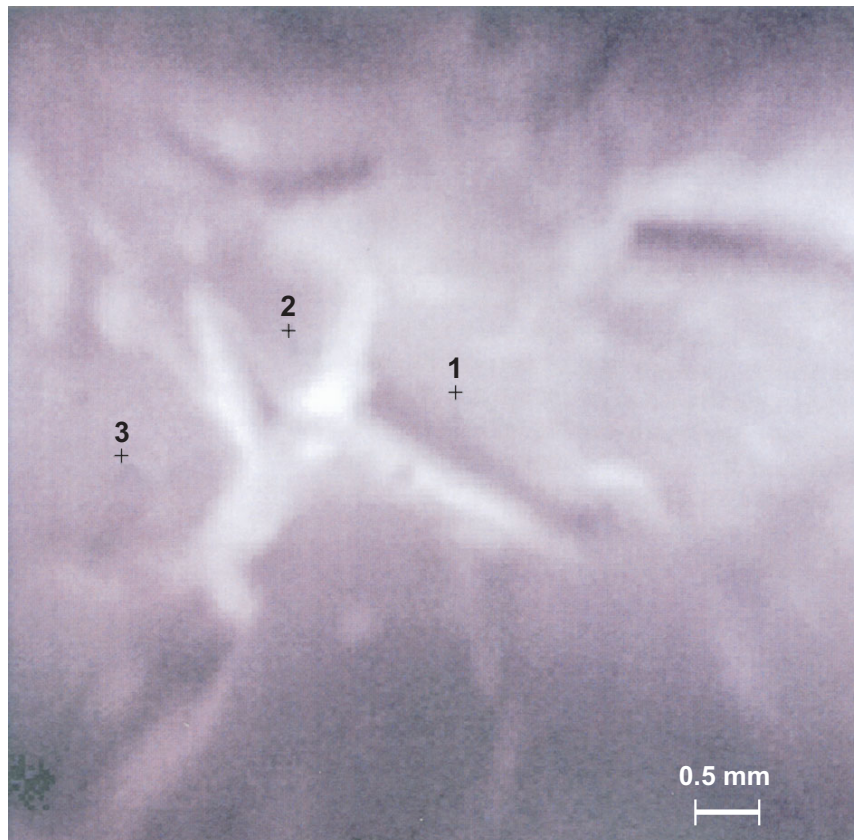


Figure 11 SXI image of the XPS measurement positions on a fracture surface

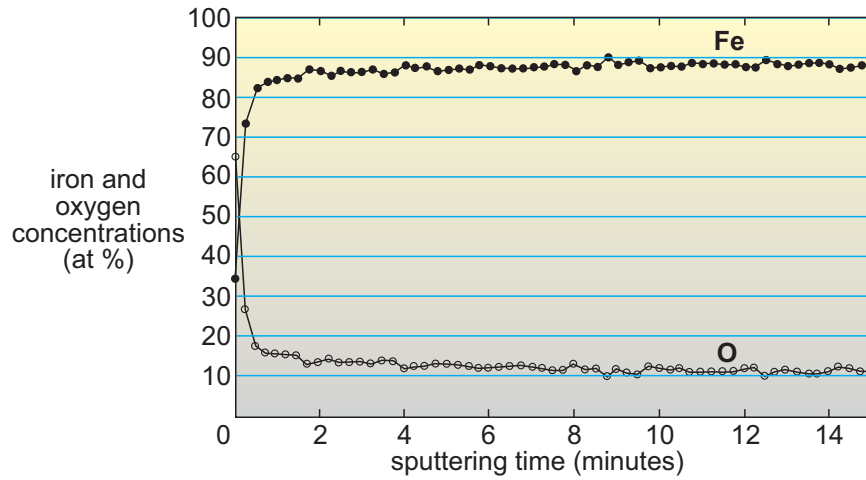


Figure 12 Representative result (position 3 in figure 11) of the XPS measurements: sputtering depth about 10^{-4} mm after 15 minutes

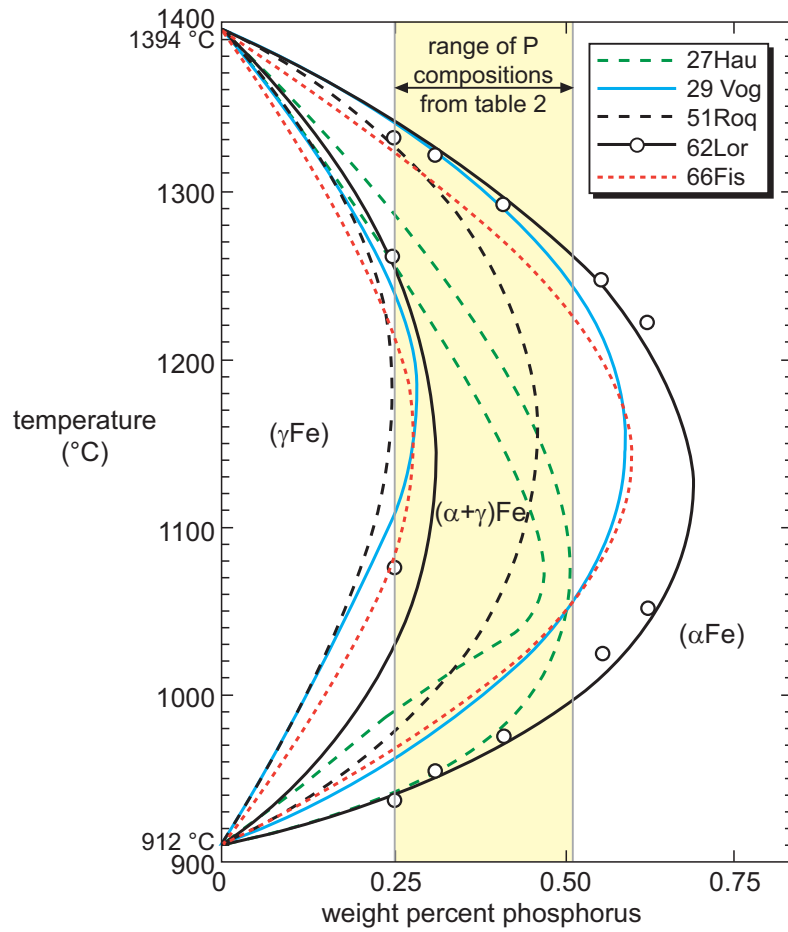


Figure 13 Detail of the iron-phosphorus binary alloy phase diagram showing the γ loop (Okamoto 1993). The positions of the $\gamma/(\alpha+\gamma)$ and $\alpha/(\alpha+\gamma)$ phase boundaries are uncertain